Rain Viewed as Relaxational Events

Ole Peters* and Kim Christensen†
Blackett Laboratory, Imperial College London, Prince Consort Road, London SW7 2BW, United Kingdom

By following an analogy to earthquakes, we demonstrate how, from the point of view of energy flow through an open system, rain is analogous to many other relaxational processes in Nature. By identifying rain events as the basic entities of the phenomenon, we show that the number density of rain events per year is inversely proportional to the released water column raised to the power 1.4. This is the rain-equivalent of the Gutenberg-Richter law for earthquakes. The event durations and the waiting times between events are also characterised by scaling regions, where no typical time scale exists. The Hurst exponent of the rain intensity signal $H = 0.76 > 0.5$. It is valid in the temporal range from minutes up to the full duration of the signal of half a year. All of our findings are consistent with the concept of self-organised criticality, which refers to the tendency of slowly driven non-equilibrium systems to evolve into a state of scale free behaviour. We note that self-organised criticality may offer an alternative to the chaos theoretic perspective on the subject of rain.

Keywords: Rain, Scaling, Relaxational Events, Self-organised criticality.

This paper is an interpretation of the fractal structures observed in a one-minute resolution precipitation time-series. Without prior knowledge of the extensive literature on fractal and multifractal observations and modelling in the atmospheric sciences, we started from a complex-systems point of view. The paper follows the chronology of the project, starting with the idea of an analogy then gathers evidence to support it and finally assesses the usefulness of the analogy.

Section I is an introduction to the concept of self-organised criticality (SOC), which will be demonstrated to be a useful frame work when thinking about atmospheric processes on a general level. It is contrasted to the only comparable approach of chaos theory.

To motivate and illustrate the use of SOC in rainfall studies, we draw an analogy in sec. II between rain showers and earthquakes, which will be elaborated throughout the paper.

Section III is a brief description of the radar measurement technique used by the Max Planck Institute in Hamburg to collect the data we analysed. A vertically pointing Doppler radar was used to collect data of very high quality with one minute resolution for 6 months.

Following the earthquake analogy set out in sec. II, we define the indispensable notion of an event in the context of rainfall (Peters, Hertlein, Christensen, 2002; Peters, Christensen 2002) and present the results obtained by employing the concept of events. We measure the probability density of events as a function of size, and find the power-law structure typical of SOC systems. We note that the range of the power law extends far beyond the sensitivity of conventional rain gauges. The waiting times between events are also power-law distributed. We explain how this is related to the fractal dimension of the binary rain-dry signal. Finally, we measure the Hurst exponent of the rain signal and obtain a non-trivial value of 0.76.

In Sec. V we conclude that SOC is a useful working paradigm. Without making any statement about the dimensionality of the dynamical attractor, SOC can provide what may be called an overall taste of the atmospheric system. SOC is in this sense a maximum ignorance approach; it is nonetheless possible to identify some of the underlying physics.

I. SELF-ORGANISED CRITICALITY

Since the first discoveries of fractal structures in nature (Richardson, 1926; Zipf, 1949) an understanding of their origins has been sought. For a long time, it was hoped that the basic description of any complex dynamical system could be reduced to a small set of simple differential equations. This hope was reinforced when it was realised that such a small set could not only reproduce smooth dynamics but also seemingly stochastic behaviour and fractality (Lorenz, 1963). With this discovery, which constitutes the birth of chaos theory, it became possible in principle to describe systems displaying highly irregular dynamics simply with a small number of first-order differential equations. Algorithms were designed to determine this number, called the dimensionality of the dynamical attractor, see e.g. Grassberger and Procaccia (1983). In practice, however, the algorithms turned out to be extremely difficult to use. In particular, for precipitation time series, it is not clear if the algorithms can be used reliably (Sivakumar, 2000). Thus, attempts to distinguish between truely stochastic and deterministic chaotic behaviour remain largely inconclusive.

With the increase of computing power in the last two

*Electronic address: ole.peters@ic.ac.uk; URL: http://www.cmth.ph.ic.ac.uk/~obp98
†Electronic address: k.christensen@ic.ac.uk; URL: http://www.cmth.ph.ic.ac.uk/kim

decades, a new perspective arose. People started to design lattice-based models defined by local interaction rules based on some straight-forward physical properties of the system to be modelled (Bak, Tang, Wiesenfeld, 1987; Christensen *et al.* 1996; Bak, Sneppen, 1993; Olami, Feder, Christensen, 1992). The models were able to reproduce the observed fractal structures and could be programmed into computers and analysed there. The simplicity now lay in the local interaction rules rather than in the overall description of the system. Note that local interaction rules will usually lead to locally confined correlation. However, for fractality, correlation on all scales is necessary, and herein lies the art of designing an SOC model. Instead of models defined by a priori low-dimensional systems of differential equations or maps, the dimensionality might or might not be reduced a posteriori by analytical tools.

This later SOC perspective was inspired by an analogy to closed systems under laboratory conditions. When tuned to the critical point of a phase transition, fractality can be observed and critical dynamical behaviour emerges. The chronology of our understanding of phase transitions indicates the path for the future: First there were observations in Nature – of magnetism – then there was a lattice-based toy model with local interaction rules (Lenz, 1920), and finally there was reductionism through analysis (Onsager, 1944).

One major difference between the recently invented models and closed systems near the critical point is the following: A closed system can only be brought to the critical region by external tuning of e.g. the temperature. The SOC models on the other hand are driven solely by their own internal dynamics. The name "self-organised criticality" is thus a reasonable choice. For a model to be applicable to the real world, self-organisation is crucial simply since there's no one around to do any tuning.

In the last 15 years many natural systems have been viewed in the SOC frame work, among them several dynamical systems, such as the earth's crust (Bak, Tang, 1989), the dynamics of a growing granular pile (Frette *et al.*, 1996), and the stick-slip behaviour of objects pulled over a frictional interface (Feder and Feder, 1991).

For all self-organised critical dynamical systems, we observe

– a slow energy input
– intermediate energy storage
– a dynamical threshold
– sudden burst-like energy releases

The atmosphere shares all of these generic dynamical properties, and we therefore felt confident to look for statistical manifestations of this similarity.

II. RAINFALL AND EARTHQUAKES

To motivate and illustrate the SOC perspective with respect to rainfall, we draw an analogy to one of the prime examples of SOC systems: The collection of tectonic plates drifting over the liquid mantle of the earth.

The picture of continental plates floating on a liquid was first suggested in 1912 by the meteorologist Alfred Wegener (1966). This fluid dynamical description of a geomorphological process was opposed for a long time by geologists but when experimentally confirmed in the late 1960s (Steward, 1990), it enabled – at least in principal – an understanding of the mechanisms at work. The main difference between meteorology and geomorphology may well be a difference in viscosity; admittedly this difference is a factor of some 22 orders of magnitude. It is not by chance that it was a meteorologist who first developed an understanding of the dynamical process responsible for earthquakes. In many ways it is similar to meteorological phenomena. In both cases, we are dealing with a system of global scale featuring spatio-temporal dynamics, while measurements are generally local. This leads to similar difficulties in identifying the overall processes that are at work. The atmosphere is more easily accessible than the mantle of the earth, and its state affects us on an everyday basis. Not surprisingly, an understanding of its dynamics began to develop much earlier than a similar understanding of the obstructed processes inside our planet.

We do not consider any of the fluid dynamical details of either of the processes. We will argue that from the point of view of energy flow, the occurrence of rain showers is similar to that of earthquakes, and is governed by similar statistics. The following two paragraphs are a – admittedly somewhat polemical – juxtaposition of the energy flows in the two systems:

Radioactive material undergoing fission in the core of the earth is constantly heating the lower part of the liquid mantle. As the upper part of the mantle is relatively cooler, convective currents arise. These currents drive the solid tectonic plates, which grind and interlock at their boundaries. Thus energy is intermediately stored in the crust in the form of tension between adjacent plates. When a friction threshold is reached in an unstable and thus susceptible environment, the system suddenly relaxes and an earthquake is triggered. The energy released in such events may devastate entire cities, or it may be equivalent to a truck passing by. Events smaller than this cannot be resolved from the background noise with today's standard seismographs.

Hydrogen undergoing fusion in the core of the sun accounts for the electromagnetic energy being radiated into space by the sun. Part of the energy is intercepted by earth. As this energy heats the lower parts of the atmosphere, it induces convective currents. 70% of the surface of the earth are water. Here, much of the solar energy is used in evaporation of water. Carried up by convection, it is intermediately stored in the form of vapor or liquid water in the atmosphere. When a saturation threshold is reached in a susceptible environment, the system suddenly relaxes and a rain shower is triggered. The energy released in such events may devastate entire cities, or it

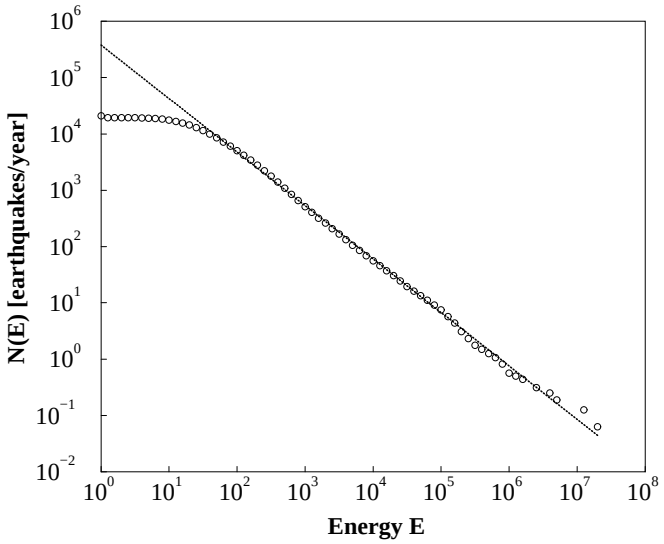

FIG. 1: The annual number of earthquakes in Southern California plotted versus the seismic moment. Data were collected from 1984 until 2000. The straight line on the double-logarithmic plot reveals the Gutenberg-Richter law. 293,405 earthquakes were observed.

may be equivalent to spilling a glass of water over the surface of dining table. Events smaller than this cannot be resolved, due to poor sensitivity, by today's standard rain gauges.

All of the characteristic features of SOC systems mentioned at the end of Sec. I are found in the atmosphere:
– it is slowly driven by solar radiation
– energy can be stored in the system
– there is a dynamical threshold related to saturation
– rain comes in cloud bursts rather than as continuous drizzle

The dynamics leading to this behaviour are similarly complex to those leading to earthquakes. For earthquakes, however, we know at least two empirical laws. One is the Gutenberg-Richter law (Gutenberg, Richter, 1944), see Fig. 1, which relates the number of earthquakes $N(E)$ in a given time interval to the released energy E.

$$N(E) \propto E^{-b}, \tag{1}$$

where $b \approx 1$.

The other is the Omori law, which states that after a main shock, the frequency of aftershocks is inversely proportional to the time elapsed since the main shock.

$$N(T) \propto T^{-\alpha}, \tag{2}$$

where $\alpha \approx 1$ (Omori, 1895).

These two laws were derived from local measurements but may be unified into one by taking into account the spatio-temporal nature of the phenomenon (Bak *et al.*, 2002).

If we wish to think of rainfall as earthquake analogues, we will have to define a rain event as the fundamental entity of the process. In the following sections we will show that acknowledging the event-like structure of rain brings to light the similarities to earthquakes almost automatically.

III. MEASUREMENT

By using radars rather than common water gathering devices, the limits on rain measurements due to evaporation, sensitivity threshold, averaging times and accessibility can be pushed considerably (Klugmann, Heinsohn, Kirtzel, 1996).

The data we used refer to a height range of 50 m vertical extension at 250 m above sea level and have been collected from January to July 1999 with the Micro Rain Radar MRR-2, developed by METEK (1998). The radar is operated by the Max-Planck-Institute for Meteorology, Hamburg, in Germany at the Baltic coast in Zingst (54.43°N 12.67°E) under the Precipitation and Evaporation Project (PEP) in BALTEX (2002). The retrieval of the rain rate is based on a Doppler spectrum analysis described by Atlas (1973). At vertical incidence, the fall velocity of a droplet can be identified with the Doppler shift. The friction force acting on a falling drop increases approximately proportional to its surface, but the gravitational force increases proportionally to its volume. Therefore, in the atmosphere, larger drops fall faster than smaller ones, and spectral bins can be attributed to corresponding drop sizes. For a given drop size, scattering cross sections can be calculated by Mie theory (Mie, 1908). Droplets are approximated by ellipsoids with known axis ratio (Beard, Chuang, 1987). The influence of the changing air density with height is considered according to Beard (1985), and standard atmospheric conditions are assumed (Weast, 1978). Attenuation of radar waves by droplets is accounted for using the observed droplet spectrum of the lowest range gate to estimate attenuation for the following one. For higher gates all observed and corrected spectra of lower layers are taken into account. Thus, from the Doppler spectrum alone one can infer the number of drops n_i of any desired volume V_i as well as their fall velocities v_i. The rain rate can be calculated instantaneously as $q(t) = \sum_i n_i V_i v_i$. In the time series we investigated, the continuous measurement is averaged over one-minute intervals, leading to one minute temporal resolution. When the signal due to rain becomes indistinguishable from the background noise at the receiver, the rain rate is defined as zero. Under the pertinent conditions, the calculated rain rate was typically $q_{min} = 0.005$ mm/h, when this happened. Note that even compared to other radars, this is a very low rain rate indeed. Of course, events at the radar's sensitivity threshold are far from being detectable by any

water-collecting pluviometer and similarly far away from what we associate with the word "rain". Nonetheless, we will consider any minute with derived $q(t) > q_{min}$ as "rain", and conversely, only if the radar fails to detect any net downward motion of water through the air, we will speak of "no rain". We will come back to this point in Sec. IV A. Especially for small rain rates the employed method is extremely powerful.

The quantitative retrieval is restricted to rain. The reflection spectra of snow and hail look very different from those of liquid water and can be identified. But in this case the method fails to calculate correct water masses. The latest version of the instrument recognises non-rain precipitation by an internal algorithm. The rain intensity data we used were calculated from measurements performed while the development of the instrument was still ongoing, and hence the raw data had to be checked manually.

IV. DATA ANALYSIS

The months January and February contain several instances of snow at our chosen measuring height of 250 m. By far the largest snow disturbance was observed on March 6, from 3:49 am until 11:38 pm. The Doppler spectra reveal that 250 m altitude was inside the melting layer, and the water column resulting from interpreting the event as rain would have been 279 mm, which is not unusual to be the total rainfall of eight weeks. In June and July, five very short periods of extremely high calculated rain rates were found. The Doppler spectra indicate two different types of drops with fall velocities at $\approx$ 4 m/s and $\approx$ 9 m/s. Comparison with meteorologic records shows that around these times, thunderstorms with hail or extreme rainfall may have caused the radar to malfunction. As in the case of snow disturbances, data gathered during these periods were excluded from the analyses in Sec. IV A and IV D. The results in Sec. IV B, and IV C, however, refer to the entire data set since the value of the rain intensity is irrelevant here. To make sure that our results are not an artifact of the observed anomalies, all analyses were also performed on the certainly clean months of April and May. No differences to the previously obtained results were observed. Due to the high resolution, not even the ranges of validity were significantly affected.

A. Event Sizes

Previous work focused on rainfall during fixed time intervals and on the statistical properties of such fluctuating rain intensities. Other studies addressed distributions of wet and dry spells, see e.g. Schmitt, Vannitsem, and Barbosa (1998). But we set out to look for similarities between rain and earthquakes. It was therefore necessary to define a different fundamental entity of rain than an arbitrarily chosen time interval (Peters, Hertlein, Christensen, 2002; Peters, Christensen, 2002). The rain event is this fundamental entity and is defined as a sequence of non-zero rain rates, and its size $M = \sum_t q(t)\Delta t$, with $\Delta t = 1$ min, is the accumulated water column during the event. The intervals of zero rain rate between events are called drought periods.

The entire agricultural sector depends on a sufficient amount of rain spread out over the months of the growth season, the individual events are only of little interest. In earthquake research the converse applies. No one depends on the average seasonal flow of energy through the earth's crust and one is mainly interested in the events. Due to this difference in anthropogenic interest, the two perspectives have been used almost entirely separately in the respective fields.

Owing to the precision and high temporal resolution of the data, an investigation into the fine structure of rain events was made possible, and the results are strikingly clear. Figure 2 shows the number density of rain events per year N(M) versus event size M on a double logarithmic plot. Note the similarity to Fig. 1. In a scaling regime $M_{min} < M < M_{max}$ extending over at least three orders of magnitude, the distribution follows the simple power law

$$N(M) \propto M^{-\tau_M}, \qquad \tau_M \approx 1.4. \tag{3}$$

This implies that a typical scale of events does not exist, and scale invariance prevails. In the scaling region, if we compare the frequency of events of size M to that of events of size kM we obtain the same fraction, independent of M. From Eq. (3), it follows that:

$$N(M)/N(k*M) = k^{\tau_M}, \qquad M \in [M_{min}, M_{max}]. \tag{4}$$

This is the typical "critical" dynamical behaviour found in SOC systems. But Fig. 2 contains even more information. For events smaller than $M_{min} \approx 5 * 10^{-3}$ mm the power law breaks down. This is indicative of a different physical process being responsible for events in this realm. Within the scaling regime, events of all sizes look alike when compared to others. Hence there is no reason to assume different physical origins. As motivated in Sec. II the common origin can be thought of as sudden relaxation, bursts of intermediately stored energy leaving the atmosphere. Where the power law breaks down, a different type of process sets in. Events smaller than M_{min} might be due chiefly to the inner dynamics of the atmosphere. Virga, drizzle that evaporates before reaching the ground, is difficult to interpret from the event perspective. Drizzle can form within clouds but immediately re-evaporate, which may be the explanation for events smaller than M_{min}. Indicated with an arrow in Fig. 2 is the typical sensitivity threshold 0.1 mm of high precision tipping bucket rain gauges. The value 0.1 mm is widely used as the definition of zero precipitation (GTOS, 2001). Given that our interpretation of the

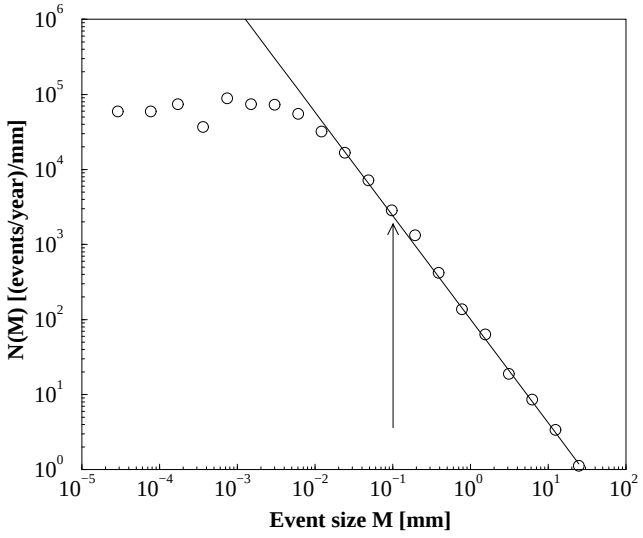

FIG. 2: The number density N(M) of rain events versus the event size M (open circles) on a double logarithmic scale. Events are collected in bins of exponentially increasing widths. The horizontal position of a data point corresponds to the geometric mean of the beginning and the end of a bin. The vertical position is the number of events in that bin divided by the width of the bin. To facilitate comparison with future work, we rescaled the number of events to annual values. The experimental data are consistent with a power law $N(M) \propto M^{-\tau_M}, \tau_M \approx 1.4$ (solid line) over at least three orders of magnitude, $M \in [M_{min}, M_{max}]$ with $M_{min} \approx 5*10^{-3}$ mm and $M_{max} \approx 35$ mm. The arrow indicates the typical sensitivity threshold of a conventional high precision tipping bucket rain gauge. Not only can we see that the radar technique is roughly 10,000 times more precise but also that a considerable fraction of rain events must be missed with conventional methods.

breakdown of the power law is correct, and every rain event with $M > 5 * 10^{-3}$ mm is actual rain, it is evident that measurements with today's standard precision simply don't see the small rain events, which are the most frequent. In our case, the events with $M_{min} < M < 0.1$ mm constitute 68% of the events within the scaling region. While these smallest 68% of all proper rain events do not account for a large amount of water, they are invaluable in addressing questions regarding the fundamental structure of rain and the actual physical processes involved. After a good decade of research, evidence for low dimensionality and the possibility of realistic disaggregation is still not conclusive. We believe that there is no substitute for high precision high resolution data, and efforts should be directed in this direction.

With the radar measurement, all rain seems to be captured and we can choose a suitable limit (M_{min}) below which events are ascribed to a different physical process. In this respect hydrologists are in a far better position than seismologists. Earthquakes below $E \approx 2$ on the Richter scale disappear in the background noise, and even part of the notorious unpredictability of earthquakes might be related to our ignorance about the low-intensity tail of the frequency distribution. For rain on the other hand, it is physically and technologically possible to detect all events at a given location.

To ascertain that we are capturing the entire physically relevant range of the observables of the process of rain, it is necessary to use observational techniques enabling us to see beyond the physical limits of rain. Results from investigations that do not fulfill this requirement cannot be conclusive and must be treated with careful scepticism. The present study suggests a reasonable maximum sensitivity threshold of around $5*10^{-3}$ mm, which is one twentieth of the commonly used threshold.

Assuming Eq. (3), we can easily calculate the number $N(M > M_1)$ of expected events exceeding a given mass M_1:

$$N(M > M_1) \propto \int_{M_1}^{\infty} M^{-\tau_M} dM = \frac{1}{\tau_M - 1} M_1^{-\tau_M+1}, \quad (5)$$

implying

$$N(M > M_2) = N(M > M_1) \left(\frac{M_2}{M_1}\right)^{-\tau_M+1}. \quad (6)$$

Since we know how many events there are with $M > M_1 = M_{min}$, Eq. (6) can be used to estimate $N(M > M_2)$, where $M_2 > M_{min}$. We observed 10 events in the largest non-empty bin ranging from 17 mm to 35 mm, but from extrapolating the power law as outlined above, we would expect another 10 in the following bin ranging from 35 mm to 70 mm. In total we would expect to see 38 events larger than the largest event that was actually observed. We therefore conclude that the sudden upper cutoff apparent in Fig. 2 is not due to the limited time of observation but rather reflects a physical limit to the process of rain at the given location. We define M_{max} as the largest event in the data set, a downpour of $M_{max} \equiv$ 35 mm of rain.

Note that the scaling regime spans 3 to 4 orders of magnitude, which is less than the Gutenberg-Richter law in Fig. 1. The fact that the scaling behaviour does not extend beyond M_{max} explains why – in contrast to earthquakes in Claifornia – rainshowers at the baltic coast are not seen as life-threatening hazards and have not been viewed in terms of events. As soon as an event exceeds a humanly managable amount of energy, it acquires a different psychological quality. The different ranges of the scaling regimes may be due to different separations of time scales. The SOC models mentioned in Sec. I (Bak, Tang, Wiesenfeld, 1987; Christensen *et al.* 1996; Bak, Sneppen, 1993; Olami, Feder, Christensen, 1992) implement an infinite separation between the driving and the relaxation time scales. This is achieved by only driving the system when all relaxation has ceased, loosely speaking corresponding to switching off the sun until all rain

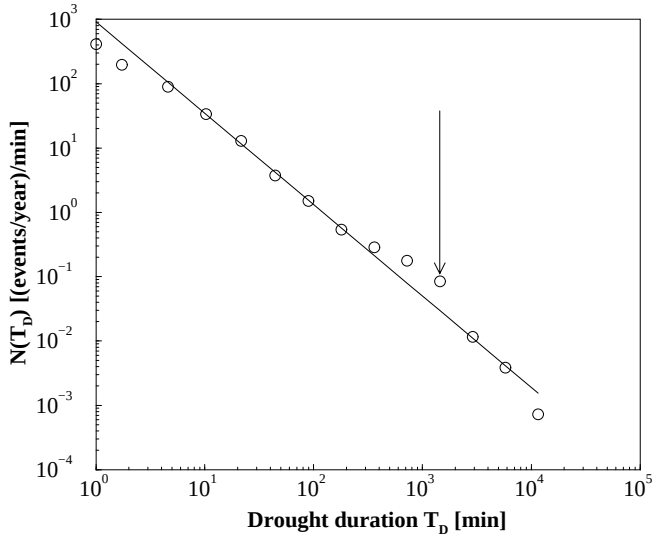

FIG. 3: The open circles show the number density $N(T_D)$ of drought periods per year versus the drought duration T_D. The solid line represents a power law approximation, with exponent $\tau_D = 1.4$, to the observed distribution. The arrow indicates one day, around which a deviation from pure power law behaviour can be observed. This is due to the daily meteorological cycle.

on earth has stopped and then switching it back on. This is not what usually happens in physical systems, instead there is a substantial but finite separation between the driving and relaxation time scales. Although typical time scales do not exist within the scaling regimes, the finite size of the earth's crust and the atmosphere make the scaling regimes themselves finite. The energy build-up before an earthquake can last from seconds to millenia, while individual relaxations take place within seconds. The respective time scales we found in the rain data are up to two weeks for the build-up and up to one day for the relaxation.

B. Drought Duration

In the last section we presented the rain equivalent of the Gutenberg-Richter law. Having thus found our initial idea confirmed, we will now focus our attention on the interoccurence times. A power law in the frequency distribution of these waiting times $N(T_D)$ would be reminiscent of the Omori law stated in Sec. I. Fig. 3 shows also this suspicion confirmed:

$$N(T_D) \propto T_D^{-\tau_D}, \qquad \tau_D \approx 1.4. \tag{7}$$

No cut-offs were apparent. The power law is a good approximation from the minimum (1 minute) all the way to the maximum (two weeks) of observed drought durations. The only observed deviation at droughts of around one day length is due to the daily meteorological cycle.

C. Fractal Dimension

A fractal is a structure displaying scale invariance of the type mentioned in Sec. IV A. Zooming into a fractal with a factor of b and then re-scaling the coordinate system with a factor of b^{d_f}, where d_f is called the fractal dimension, leaves the structure unchanged. Fractals often occur naturally, in which case the unchanged property is usually a statistical one. The rain data are from one fixed location but they span a long period of time. We define a binary signal – either rain or drought – and determine its fractal dimension in time, using the box counting method: Different lengths l of time intervals (boxes) are used to cover the rainy sections on the time axis. The number of boxes $n(l)$ needed to cover the rain is proportional to l^{-d_f}.

The results are displayed in Fig. 4. In the double-logarithmic plot we find an S-shaped curve. The dashed lines indicate the trivial slope, $d_f = 1$, while the solid lines in the central scaling regime have non-trivial $d_f \approx 0.55$ and $d'_f \approx 0.42$.

The only way to obtain a non-trivial fractal dimension is to have no typical drought duration at all. Mathematically, this scale-freedom is represented by the power-law distribution of drought durations. The number of boxes needed to cover the rain signal will be the true rain duration plus the time spanned by droughts that are shorter than the box size (these will be overlooked), all divided by the box size. Hence, apart from a constant, representing 8% of the total time, the time T_c spanned by the boxes to cover the rain will increase with l as $T_c = \int_0^l N(T_D)\, T_D\, dT_D \propto \int_0^l T_D^{-1.42}\, T_D\, dT_D$, which is implied by Fig. 3. Evaluating the integral we have $T_c \propto l^{0.58}$. The number of boxes needed is $T_c/l = l^{-0.42}$. In this sense a fractal relation like the one shown in Fig. 4 could be a consequence of a power-law distribution of drought durations like in Fig. 3. The values we measure suggest that there is more to the rain - no rain signal than only the power law of interoccurrence times. Deducing the fractal dimension from the drought distribution only, we would expect a value of 0.42. But we observe 0.55, and the difference appears to be significant.

The scaling regime extends from a lower limit around 10 minutes to an upper breakdown near 3 to 4 days. While one might expect the fractal regime to span further for longer time series, the analysis of a 30 year time-series from Uccle (Schmitt, Vannitsem, Barbosa, 1998) suggests that the observed breakdown is not an artifact of the shortness of our data-set. The authors find the same value $d_{fS} \approx 0.55$ (where S indicates the first author of the study) and place the cut-off at 3.5 days, which coincides with our values. Apparently, the correlation that gave rise to the fractal relation does not hold for longer than

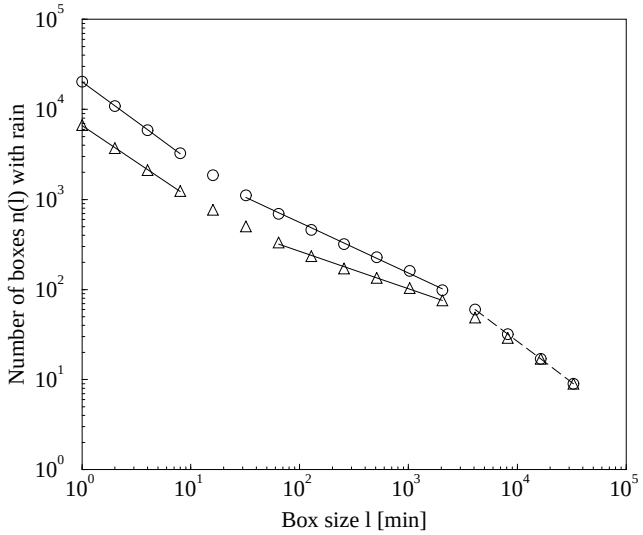

FIG. 4: The number of time intervals (boxes) needed to cover the rain versus the box size. The fractal dimension d_f is minus the slope of this graph in a double logarithmic plot. Using the radar sensitivity as our threshold value to distinguish between rain and drought (circles), we obtain $d_f \approx 0.55$ in a scaling regime spanning 2 orders of magnitude. Introducing a higher threshold of 2.1 mm/h, corresponding to 420 times the sensitivity threshold of the radar, we observe a lowering of the fractal dimension to $d'_f \approx 0.42$ (triangles). For values of l to the left of the central scaling regime, it assumes the value $d_f \approx 0.88$ without an artificial threshold and $d'_f = 0.81$ with 2.1 mm/h threshold. To the right of the central scaling regime the fractal dimension approaches the trivial value $d_f = 1$.

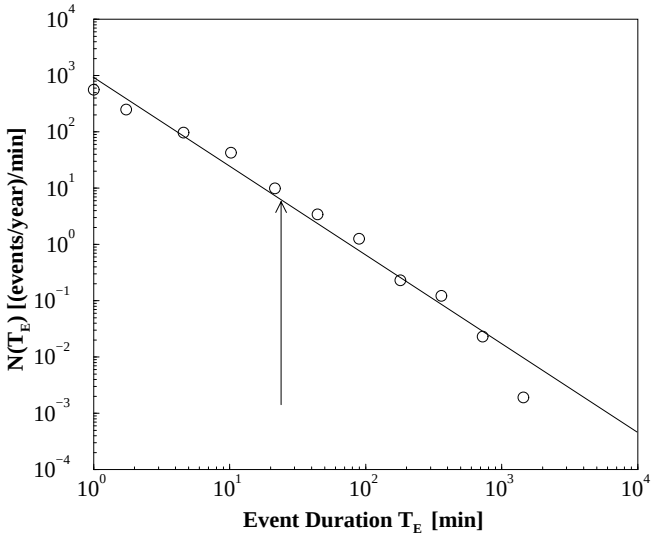

FIG. 5: The number of observed rain events vs. their duration approximates to a power law, suggesting that there is no "typical" event duration. The most frequent event duration we observed was 1 minute. The distribution of event durations is not peaked anywhere, thus no characteristic time scale can be identified. In particular, the average duration of 24 min is in no significant sense different from any other duration between 1 and 700 min.

3.5 days. Investigation of time series from Denmark with 1-day resolution, collected from 1876 until 2000 (Laursen *et al.*, 2001) does not suggest that the power law for droughts holds for drought durations exceeding the upper cut-off in the fractal dimension.

The explanation for the upper cutoff of the fractal regime may be that the typical duration of a frontal system moving in from the Atlantic is of the order of 3 days. Measured rain parameters will not belong to the same frontal system if the measurements are temporally separated by significantly more than three days. The lower breakdown around 10 min could not be observed in the Uccle time series since there the temporal resolution was only 10 minutes. Other studies (Lavergnat, Golé, 1998; Olsson, Niemczynowicz, Berndtsson, 1993) show that there is no general agreement regarding the cause of the 10-minute breakdown and the value of the fractal dimension. Some of the controversy regarding the fractal dimension can, however, be resolved.

Olsson *et al.* find $d_{fO} \approx 0.37$ and place the position of the lower breakdown at 45 minutes. They note that 45 minutes is the average duration of a single event and identify the average duration with the typical duration. Given the power-law distribution of event duraions shown in fig. 5 we dare to question the validity of this identification. 45 minutes is certainly not the most frequent rain event duration. The authors also note that the value of the fractal dimension changes with the sensitivity of the instrument. Introducing a threshold, mimicking a less sensitive rain gauge, has the effect of lowering their value of $d_{fO} \approx 0.37$. The tipping bucket rain gauge employed by them has a sensitivity threshold of 0.035 mm. Given 1 minute temporal resolution, this corresponds to an intensity of 2.1 mm/h. For comparison, we introduced a threshold corresponding to the sensitivity of their instrument and found the value of the fractal dimension lowered to $d'_f \approx 0.42$, which may be considered consistent with Olsson *et al.*'s result. As we lower the threshold, i.e. effectively improve the sensitivity of our instrument, the fractal dimension changes continuously until it reaches our value of $d_f \approx 0.55$ at a threshold around 0.2 mm/h, corresponding to a smallest detectable event of 0.003 mm. This one tenth of Olsson's gauge's sensitivity threshold and is near the value of the breakdown of the power law event size distribution. Improving the sensitivity further doesn't change the fractal dimension any more.

The time series used by Schmitt *et al.* has a temporal resolution 10 times less precise than that of Olsson *et al.* The benefit of this low resolution is, given the simple idea of collecting water in a container, that 10

times lower intensities can be identified with the correct time interval. There is a trade-off between temporal resolution and sensitivity, and it seems that Olsson *et al.* bargained for too much temporal resolution, losing the necessary sensitivity. Schmitt *et al.*, on the other hand, seem to have hit exactly the maximum acceptable sensitivity threshold, using the tipping bucket technique at – but not beyond – its physical limits.

Lavergnat and Golé used an instrument measuring the arrival times of individual rain drops with a temporal resolution of 1 ms. They do not observe a breakdown of the scaling regime anywhere near 10 minutes. Instead, the scaling behaviour change as soon as the box size becomes smaller than the shortest interoccurrence time between two raindrops ($\approx$ 100 ms). The value obtained for the fractal dimension $d_{fL} \approx 0.82$. Very similar values are found by Olsson *et al.* ($d_{fO} \approx 0.82$) and ourselves ($d_f \approx 0.88$, $d'_f \approx 0.81$) in the temporal range, boxsize $l < 10$ min, below the lower breakdown of the central scaling regime. The temporal resolution of Lavergnat and Golé's instrument of 1 ms leads to the process being viewed as a point process of rain drop arrival times. The fact that they do not see a central scaling regime may be related to this point-process perspective.

We interpret these result as another sign of having captured the whole range of sizes of rain events. The discrepancies between results obtained by Olsson *et al.*, Schmitt *et al.* and ourselves can be resolved considering the physical constraints of the different measurement techniques. Lavergnat and Golé's findings need further clarification. Measurements with a sensitivity threshold greater than 0.003 mm will yield results reflecting the instrument's sensitivity rather than properties of the dynamical system producing the rainfall. Similar multifractal behaviour has been observed in earthquake models (Olami, Christensen, 1992).

We are unsure as to how to interpret the lower breakdown. Clearly there must be a lower breakdown somewhere, and we expect it to occur where the particular kind of correlation that gave rise to the fractality on hourly to daily time scales ceases. The lower breakdown indicates that 10 min to 45 min is a time scale which is special, and it must be related to a physical process. The microphysical processes of coagulation that trigger a cloud to release its water content take place on this time scale. Starting with typical small cloud droplets with radius $r \approx 10^{-3}$ mm, the process of stochastic collection during which small droplets merge to form rain drops of appreciable fall velocity takes roughly $10 - 30$ min under typical warm cloud conditions (Houze, 1993). It is possible that coagulation starts at a certain level inside a cloud and then pauses at that level before a single drop has left the cloud. If it then starts again, it is possible that on the ground we observe two layers of rain separated by a vertical distance corresponding to up to $\approx$ 10 min fall time. While this seems like two different events, from the cloud's perspective it is really only one, since the process of releasing water did not stop at any moment everywhere within the cloud. Effects of motion of the cloud relative to the ground are not included in these considerations. It is unlikely that the 10 minute time scale is a result of the employed measurement technique as suggested by Lavergnat and Golé (1998). The radar measurement is entirely differrent from the tipping bucket used by Olsson *et al.* (1993) and Schmitt *et al.*, yet the same cut-off is observed.

D. Hurst Exponent

In an attempt to determine the necessary size of a water reservoir that would never empty nor overflow, Hurst (1965) considered an incoming signal q(t), corresponding to the rain intensity in our case, that causes the level of a reservoir to rise or fall. Using our data, the deviation from the average water level in an imaginary reservoir would be

$$X(t,\tau) = \sum_{u=0}^{t} (q(t) - \langle q \rangle_\tau)\, \Delta t, \tag{8}$$

where Δ t = 1 min and

$$\langle q \rangle_\tau = \frac{1}{\tau} \sum_{t=1}^{\tau} q(t). \tag{9}$$

The quantity $-\langle q(t) \rangle_\tau$ in Eq. (8) can be thought of as an average outflux from the reservoir and insures that for any period τ the water level starts and ends at zero. Overall trends during the interval τ are thus eliminated. Figure 6 shows $X(t,\tau)$ as derived from the rain data.

The range of water levels the reservoir has to allow for is then given by

$$R(\tau) = \max_{1 \le t \le \tau} X(t,\tau) - \min_{1 \le t \le \tau} X(t,\tau). \tag{10}$$

Hurst determined the dimensionless ratio $R(\tau)/S(\tau)$ as a function of τ, where $S(\tau)$ is the standard deviation of the influx $q(t)$ in the period τ. It can be shown that if $q(t)$ is any random signal with finite variance (Feller, 1951), this ratio increases as

$$R(\tau)/S(\tau) \propto \tau^H, \tag{11}$$

where $H = 1/2$ is called the Hurst exponent. Hurst's analysis on data from the Roda gauge at the Nile, however, yielded a different exponent of $H \approx 0.77$. This unexpected result is commonly interpreted as a sign of persistence in the signal, or even as correlation. The exponent obtained from performing the same analysis on our data is $H \approx 0.76$ (see Fig. 7). Hence, the fluctuating rain rate alone produces an anomalous Hurst exponent, and the result obtained by Hurst is valid not only for the range of 1 year $< \tau <$ 1080 years that he considered but in fact also holds for $\tau =$ a few minutes to $\tau = 1/2$ year.

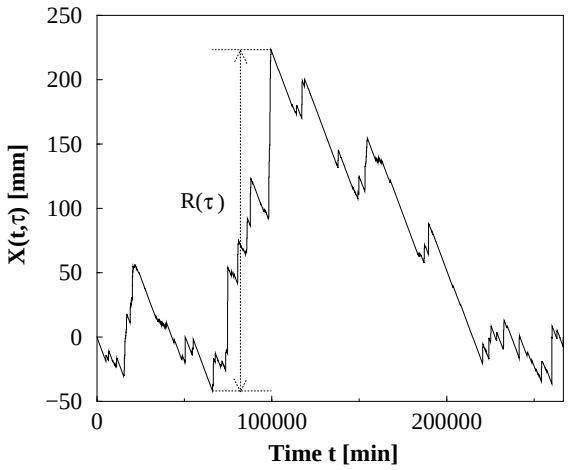

FIG. 6: Water level $X(t,\tau)$ in mm in an imaginary reservoir for τ=266,611 min as derived from the Zingst data. During drought periods, a constant, slow decrease in the water level is observed, whilst during rain events the water level increases rapidly. The necessary size of a sufficiently large reservoir is given by the range indicated by a dashed line.

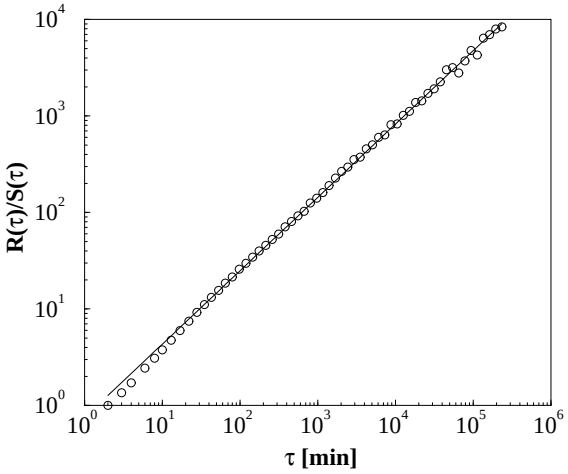

FIG. 7: The dimensionless ratio $R(\tau)/S(\tau)$ versus τ (open circles) shown on a double logarithmic scale. The slope of the fitted straight line (solid) reveals the anomalous Hurst exponent: $R(\tau)/S(\tau) \propto \tau^H$ with $H \approx 0.76$. The data deviate from the power law fit below $\tau \approx 10$ min in the lower limit, but no upper limit of the relation is observed.

Interestingly, the Hurst exponent deviates from this relation for $\tau < 10$ min, which is of the same order as the observed short-time trivial regime of the fractal dimension.

To understand more precisely what is actually measured by the Hurst exponent, we applied the same method to a signal generated by swapping events and droughts at random. We kept the sizes and durations of rain events and droughts as determined from the real data and pasted them one after the other in random order. The Hurst exponent was ınot altered by this procedure. In this sense it is not a measure of correlation since it is not affected by the order in which events occur. In exactly what sense it measures persistence is part of our ongoing research.

V. CONCLUSION

New insight into the working of rain can be gained by defining rain events, which can be regarded as energy relaxations similar to earthquakes. Taking this perspective, scale-free power-law behaviour is found to govern the statistics of rain over a wide range of time- and event size scales. Where clear deviations from the observed power laws and fractal dimensions are found, the limits and peculiarities of the underlying dynamical system become apparent, and physical insight is gained. Our findings suggest that rain is an excellent example of a self-organised critical process. Rain is a ubiquitous phenomenon, and data collection is relatively easy. It is therefore well suited for work on SOC, and we believe that atmospheric research will benefit from research on self-organised criticality and vice versa. As a general perspective on the subject, SOC offers an alternative to chaos theory while supporting the view that the atmospheric system enters a dynamical attractor which is characterised by scale freedom. Although traditionally starting with high dimensionality, it makes no explicit statement about the dimensionality of the attractor. For our purposes, the remote sensing technique employed by the MRR-2 has proved extremely powerful. It is our impression that a precondition for gaining a deeper understanding of the atmosphere as a complex dynamical system is the gathering of comprehensive data sets with high precision instruments such as the MRR-2. The radar achieves outstanding precision in the low-intensity limit and is capable of even higher temporal resolution than 1 min, limited only by the finite vertical extension of the scattering volume. Comparison with data from other measuring sites, especially from warmer regions without snow and regions with more periodic climate would be useful in order to answer questions regarding the universality of the observed features. Analysis of data from a network of high-precision radars with emphasis on the spatio-temporal nature of the processes would be particularly instructive.

VI. ACKNOWLEDGMENTS

We would like to thank the group in Hamburg and especially G. Peters for their contributions to the success of the project. We gratefully acknowledge the financial support of U.K. EPSRC through grant nos. GR/R44683/01 and GR/L95267/01. The MRR-2 data collection was supported by the EU under the Precipitation and Evaporation Project (PEP) in BALTEX.

[1] Atlas, D., Srivastava, R.C., and Sekhon, R.S., (1973). Doppler Radar Characteristics of Precipitation at Vertical Incidence. Rev. Geophys. Space Phys. **11**, 1-35 .

[2] Bak, P. and Sneppen, K., 1993. Punctuated equilibrium and criticality in a simple model of evolution. Phys. Rev. Lett. **71,** 4083-4086.

[3] Bak, P. and Tang, C., 1989. Earthquakes as a self-organised critical phenomenon. J. Geophys. Res., **94**, 15635-15637.

[4] Bak, P., Tang, C., Wiesenfeld, K., 1987. Self-organized criticality – an explanation for 1/f noise. Phys. Rev. Lett. **59** 381-384.

[5] Bak, P., Christensen, K., Danon, L., Scanlon, T., 2002. Unified scaling law for earthquakes. Phys. Rev. Lett. **88**, 178501, 1-4.

[6] BALTEX, information on the BALTEX project is available from the website http://w3.gkss.de/baltex/.

[7] Beard, K. V., 1985. Simple altitude adjustments to raindrop velocities for Doppler Radar analysis. J. Atmos. Oceanic Technol. **2**, 468-471.

[8] Beard, K. and Chuang, C., 1987. A New Model for the Equilibrium Shape of Raindrops. J. Atmos. Sci. **44** (11) 1509-1524.

[9] Christensen, K., Corral, A., Frette, V., Feder, J., Joessang, T., 1996. Tracer dispersion in a self-organized critical system. Phys. Rev. Lett. **77**, 107-110.

[10] Feder, H.J.S. and Feder, J., 1991. Self-organized criticality in a stick-slip process. Phys. Rev. Lett. **66** 2669-2672.

[11] Feller, W., 1951. The Asymptotic Distribution of the Range of Sums of Independent Random Variables. Ann. Math. Stat. **22**, 427-432.

[12] Frette, V., Christensen, K., Malthe-Sørenssen, A., Feder, J., Jøssang, T., Meakin, P., 1996. Avalanche dynamics in a pile of rice. Nature **379**, 49-52.

[13] Grassberger, P., Procaccia, I., 1983. Measuring the strangeness of strange attractors. Physica D **9**, 189-208.

[14] GTOS, Global Terrestrial Observation System: Requirements for precipitation measurements http://www.fao.org/gtos/tems/variable_list.jsp (2001).

[15] Gutenberg, B., and Richter, C.F., 1944. Frequency of Earthquakes in California. Bull. Seismol. Soc. Am. **34**, 185-188.

[16] Houze, R.A. Jr. *Cloud Dynamics* (Academic Press Inc, San Diego, 1993).

[17] Hurst, H.E., *Long-Term Storage: An Experimental Study* (Constable & Co. Ltd., London, 1965).

[18] Klugmann, D., Heinsohn, K., Kirtzel, H.J. A low cost 24 GHz FM-CW Doppler radar rain profiler. Contr. Atmos. Phys. **69**, 247-253 (1996).

[19] Laursen, E.V., Larsen, J., Rajakumar, K., Cappelen, J., Schmith, T., Observed Daily Precipitation, Temperature and Cloud Cover for Seven Danish Sites, 1876-2000. Technical report from DMI. Data available from http://www.dmi.dk/dmi via "publikationer", "tekniske rapporter", No. 01-10 (2001).

[20] Lavergnat, J. and Golé, P., 1998. A stochastic raindrop time distribution model. J. app. meteorol. **37** 805-818.

[21] Lenz, W., Phys. Zeitschrift **21**, 613 (1920)

[22] Lorenz, E.N., 1963. Deterministic Nonperiodic Flow. J. Atmos. Sci. **20** 130-141.

[23] METEK, MMR-2, Physical Basis, pp. 21 (1998). Available from METEK GmbH, Fritz-Straßmann-Straße 4, D-25337 Elmshorn, Germany.

[24] Mie, G., Beitrge zur Optik trber medien, speziell kolloidaler Metall-Lsungen. Ann. Phys. **25**, 377-445 (1908).

[25] Olami, Z., Christensen, K., 1992. Temporal correlations, universality, and multifractality in a spring-block model of earthquakes. Phys. Rev. A **46** 1720.

[26] Olami, Z., Feder, H.J.S., Christensen, K., 1992. Self-organized criticality in a continuous, nonconservative cellular automaton modelling earthquakes. Phys. Rev. Lett. **68**, 1244-1247. 0

[27] Olsson, J., Niermczynowicz, J., and Berndtsson, R., 1993. Fractal analysis of high-resolution rainfall time series. J. Geophys. Res. **98** (D12) 23,265-23,274.

[28] Omori, F., 1895. On the After-shocks of Earthquakes. J. College Sci. Imper. Univ. Japan **7** 111-200.

[29] Onsager, L., 1944. A Two-Dimensional Model with an Order-Disorder Transition Phys. Rev. **65**, 117-149.

[30] Peters, O., Hertlein, C., Christensen, K., 2002. A complexity view of rainfall. Phys. Rev. Lett. **88**, 018701, 1-4 (2002).

[31] Peters, O., Christensen, K., Rain: Relaxations in the sky. Phys. Rev. E **66** , 036120 (2002)

[32] Richardson, L.F. Atmospheric Diffusion on a Distance-Neighbour Graph. Proc. R. Soc. A **110**, 709-737 (1926).

[33] Schmitt, F., Vannitsem, S., Barbosa, A., 1998. Modelling of rainfall time series using two-state renewal processes and multifractals. J. Geophys. Res. **103**, D18 23181-23193.

[34] Sivakumar, B., 2000. Chaos theory in hydrology: important issues and interpretations. J. Hydr. **227**, 1-20.

[35] Steward, J.A., *Drifting Continents and Colliding Paradigms* (Indiana University Press, 1990)

[36] Weast, R.C., *CRC Handbook of Chemistry and Physics 58th edition*, (CRC Press Cleveland, 1978).

[37] Wegener, A., *The Origin of Continents and Oceans* (Dover, New York, 1966)

[38] Zipf, G.K. *Human Behaviour and the Principle of Least Effort* (Addison-Wesley, Cambridge MA, 1949).